

# Electrostatic-control performance measurement of the inertial sensor with a torsion pendulum

H B Tu, Y Z Bai, Z B Zhou<sup>1</sup> and J Luo

School of Physics, Huazhong University of Science and Technology, Wuhan 430074, P.R. China

E-mail: zhouzb@mail.hust.edu.cn

**Abstract.** An electrostatic-controlled torsion pendulum was used to simulate the operation of the inertial sensor in flight. The twist motion of the proof mass was monitored by a capacitance transducer and was controlled by an electrostatic actuator. The influences of the parasitic coupling of the capacitance transducer, the magnetic field, and the translation motion coupling were measured. The torque noise of the controlled pendulum came to about  $6 \times 10^{-13} \text{ N m Hz}^{-1/2}$  from 2 mHz to 0.1 Hz, mainly limited by the translation-rotation coupling and the back action of the capacitance sensor, which could be suppressed by extending the gap of the capacitance sensor.

## 1. Introduction

High precision inertial sensors play a paramount role in gravitational experiments in space [1-3]. These inertial sensors can be classified as two operation modes. In one mode the sensors act as a free-falling reference to guide the micro-Newton thrusters to compensate the non-gravitational forces received by the spacecraft, namely the drag-free control, such as those in the LISA and GOCE missions. In the other mode the sensors act as an accelerometer to measure the accelerations of the spacecraft or the expected forces, such as those in the CHAMP, GRACE, and MicroSCOPE missions. In both modes the proof masses (PMs) should be isolated from any residual disturbances. For LISA mission, the spurious accelerations of the PM should be smaller than  $3 \times 10^{-15} \text{ m s}^{-2} \text{ Hz}^{-1/2}$  from 0.1 mHz to 0.1 Hz, which is a tremendous challenge for ground-based measurement.

For high precision inertial sensors, the performance verification on ground is limited by 1 g Earth's gravity acceleration. One scheme is to use high voltage to levitate the PM, and ONERA succeed to develop the STAR and SuperSTAR accelerometers using this scheme. However, the experimental level was limited to  $10^{-9} \text{ m s}^{-2} \text{ Hz}^{-1/2}$  due to the very stiff coupling of the high electric field and seismic noises [4]. Another scheme is to suspend the PM by a thin fiber to act as a torsion pendulum or balance. A torque resolution better than  $10^{-14} \text{ N m Hz}^{-1/2}$  has been achieved by several groups with torsion balance or pendulum [5-7]. University of Trento had made plentiful progress to investigate the residual disturbances of the PMs for LISA and LISA Pathfinder with the torsion pendulum [7-10].

The torsion pendulum can be used not only to investigate the residual disturbances of the PM based on its high sensitivity to the weak force, but also to simulate the operation of the inertial sensor in flight based on the weak coupling of the fiber [11, 12]. For the second application, the gap between the electrodes and the PM is in general smaller than 1 mm, and the negative stiffness  $k_e$  due to the capacitance transducer is much larger than that of the fiber  $k_f$ . It means that the torsion pendulum is

unstable if without the feedback control. It is beneficial to estimate the performance of the electrostatic actuator for controlling the non-sensitive motions of the PM in the LISA mission, and to investigate the cross coupling between the non-sensitive and sensitive motions of the PM and the drag-free control on ground. An electrostatic-controlled torsion pendulum was developed to investigate the performance of the inertial sensor in our laboratory, and the progress was outlined.

## 2. Experimental setup

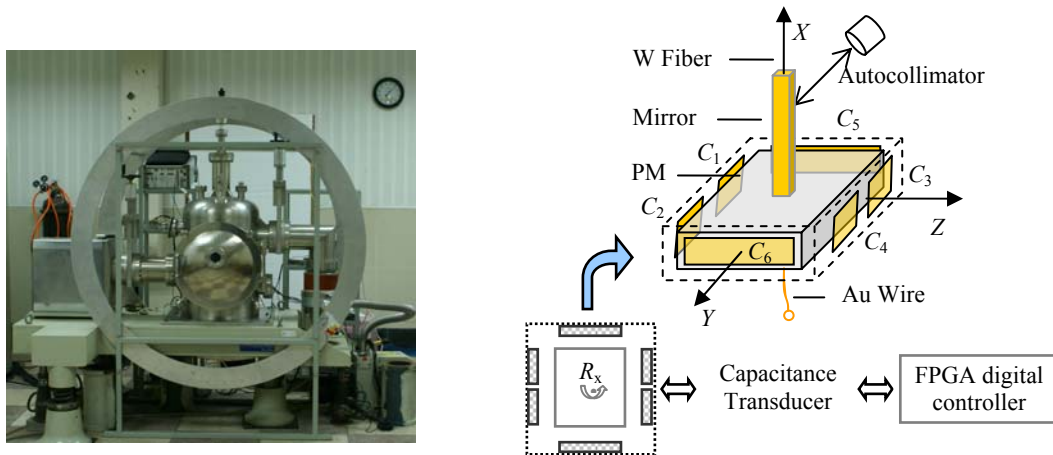


Figure 1 Left: Photo of the experimental setup; Right: Schematic diagram of the electrostatic-controlled torsion pendulum. It consists of a sensor head, capacitance transducer and a digital controller. Six electrodes are used to measure both the translation and the twist motions of the PM, and control the twist motion.

The schematic diagram of the electrostatic-controlled torsion pendulum is shown in figure 1. A titanium cuboid PM of about  $4\text{ cm} \times 4\text{ cm} \times 1\text{ cm}$  combined with a mirror was suspended by a  $25\text{ }\mu\text{m}$  tungsten fiber with a length of about  $40\text{ cm}$ . A  $5\text{ }\mu\text{m}$  Au wire with a length of about  $4\text{ cm}$  was used to discharge the PM, and its elastic coefficient was measured as  $4.2 \times 10^{-11}\text{ N m rad}^{-1}$  by comparing the free oscillating periods of the torsion pendulum with and without the discharge wire, which was about 300 times smaller than that of the suspension tungsten fiber. The total mass of the pendulum was about  $78\text{ g}$  and the moment of inertia was about  $1.995 \times 10^{-5}\text{ kg m}^2$ . The free oscillation period  $T_0$  of the pendulum with the discharge wire was  $(248.4 \pm 0.9)\text{ s}$ , and the quality factor  $Q$  was about 2800 under the vacuum of  $2 \times 10^{-5}\text{ Pa}$ . The total elastic coefficient  $k_f$  was  $(1.28 \pm 0.01) \times 10^{-8}\text{ N m rad}^{-1}$ .

The electrode frame was made of Au-coated glass-ceramics, which was mounted on a six degree-of-freedom manipulator. Three pairs of electrodes were used not only to measure the  $Y, Z$  translations and twist of the PM, but also to control the twist of the PM and investigate the twist-translation coupling. The equilibrium capacitance gaps  $d_0$  were about  $150\text{ }\mu\text{m}$ .  $C_1 \sim C_4$  and  $C_5 \sim C_6$  were about  $4.9\text{ pF}$  and  $13.3\text{ pF}$ , respectively. A capacitance transducer circuitry based on the AC capacitance and transformer bridge [11, 12], combined with a digital control loop based on a field-programmable-gate-array (FPGA), was developed. The noise of the capacitance transducer was  $2 \times 10^{-6}\text{ pF Hz}^{-1/2}$  from  $10\text{ mHz}$  to  $1\text{ Hz}$ , and was dominated by  $f^{-1}$  noise at the frequency range below  $10\text{ mHz}$ .

Four coils were used to investigate the effects of the magnetic field. A pair of large Helmholtz coils with diameters of about  $1.6\text{ m}$  was symmetrically set outside the vacuum chamber along the  $Y$  axis, as shown on the left in figure 1, while two small coils were mounted near the electrodes inside the chamber along the  $Z$  axis. Each small coil with a diameter of about  $27\text{ mm}$  and turn number of 130 was made of  $0.4\text{ mm}$  enameled copper. In order to distinguish the torque from the susceptibility and residual dipole moment of the PM, both of the small coils were symmetrically departed  $20\text{ mm}$  along the  $Y$  axis and  $61.5\text{ mm}$  along the  $Z$  axis away from the center of the PM, as shown in figure 2. Four heaters were set close to the center of each electrode along the  $Z$  axis to investigate the effects of the

temperature, and four temperature sensors were employed to measure temperature variations. The resistance of each heater was about  $5 \Omega$ . An aluminum shield box with a thickness of about 4 mm was used to partly shield the PM from the disturbances of residual gas and heat flow.

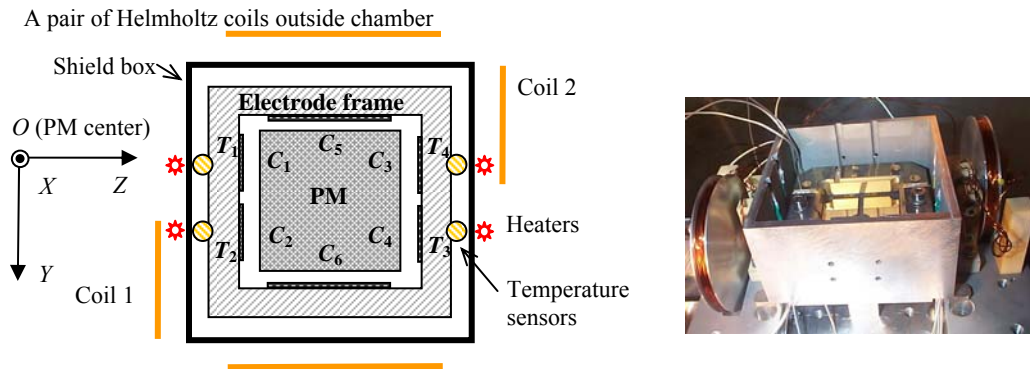


Figure 2 Left: Schematic diagram of the residual disturbances experiment. Right: Photo of the layout in chamber.

### 3. Current Experimental Results

#### 3.1. Torque sensitivity calibration

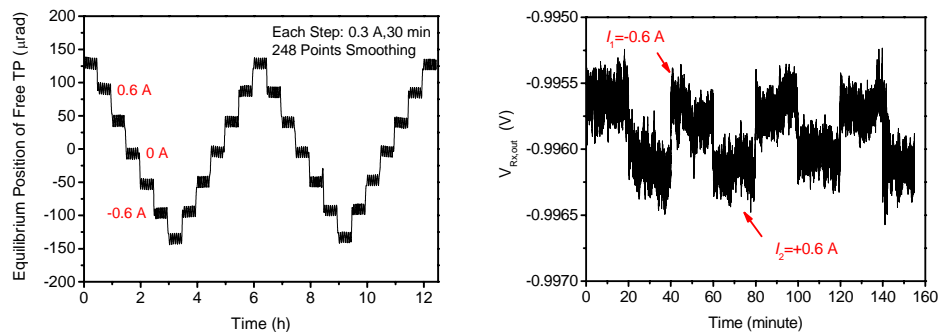


Figure 3 Left: Position variation of the torsion pendulum in free oscillation mode. Right: Feedback voltage variation in electrostatic-controlled mode.

A torque originating from the interaction of the remnant dipole moment  $\mathbf{M}_T$  of the PM with an applied magnetic field  $\mathbf{B}$  induced by the Helmholtz coils can be employed to calibrate the torque sensitivity of the electrostatic actuators. The magnetic torque is firstly measured based on the elastic torque of the suspending fiber in the case of the free oscillation pendulum, where the electrode frame was dropped below the PM by driving the manipulator, and then the sensitivity of the electrostatic actuator can be determined by the same magnetic torque under the control mode. In the free oscillation mode, when the currents through the Helmholtz coils varied from  $-0.6 \text{ A}$  to  $0.6 \text{ A}$ , the twist variation of the pendulum was  $(180.6 \pm 5.1) \mu\text{rad}$  as shown on the left in figure 3, which was simultaneously monitored by an autocollimator with a resolution of  $0.1 \mu\text{rad Hz}^{-1/2}$ . In the control mode, the feedback voltage variation was  $(-0.40 \pm 0.07) \text{ mV}$  as the same ( $\pm 0.6 \text{ A}$ ) currents were alternately applied through the coils, as shown on the right in figure 3. Therefore, the torque sensitivity could be determined as  $S_{Nm} = (1.73 \pm 0.31) \times 10^8 \text{ V (N m)}^{-1}$ , which was in good agreement with the theoretical estimation given by  $d_0 / (V_b \sum_{i=1}^4 C_i)$ , here  $V_b$  is a  $5 \text{ V}$  DC bias voltage for linearizing the electrostatic actuators. An AC  $V_b$  would be considered to apply to the PM in order to suppress the charge coupling in the further experiments. The twist angle synchronously recorded by the autocollimator was less than

1  $\mu\text{rad}$ , which contributed an uncertainty of  $10^{-14}$  N m. Furthermore, the magnetic field variation, which generated by the Helmholtz coils from -0.6 A to 0.6 A, was directly measured as about -101.4  $\mu\text{T}$  along  $Y$  axis in the space of the PM by a magnetometer with a precision of 10 nT. Then the  $Z$  component  $\mathbf{M}_{tz}$  of the residual dipole moment of the PM could be estimated as  $(-2.3 \pm 0.4) \times 10^{-8}$  A m<sup>2</sup> based on the coupling  $\Delta\boldsymbol{\tau} = \mathbf{M}_r \times \mathbf{B}$ .

### 3.2. The parasitic stiffness measurement

The parasitic stiffness  $k_e$  of the capacitance transducer is a very important parameter for determining the parameters of the control loop and estimating the back-action torque noise of the pendulum. For the twist of the torsion pendulum  $R_x$ , it can be expressed as

$$k_e \approx -\frac{(3b^2 + 3ad_0 + h^2)V_T^2}{12d_0^2} \sum_{i=1}^6 C_i \quad \text{with } V_T^2 = V_{R_{x,\text{out}}}^2 + V_b^2 + V_p^2/2 \quad (1)$$

where  $a$  is the side length of the PM,  $b$  is the distance between the adjacent electrodes,  $h$  is the width of the electrode,  $V_{R_{x,\text{out}}}$  and  $V_p$ , respectively, are the control voltage and a pumping voltage with a frequency of 100 kHz and an amplitude of 4 V applied to the PM. The twist position of the PM relative to the frame was periodically set by the FPGA unit. Thanks to the electrostatic control, the PM was controlled to follow up with the setting position. The electrostatic-controlled torque is equal to the torque induced by  $k_e$  if neglecting the effect of the suspension fiber, which is given by

$$\Delta V / S_{Nm} = k_e \times \Delta\theta. \quad (2)$$

The error signal variation of each step was 0.01V, which corresponded to the twist angle was  $(12.4 \pm 0.2)$   $\mu\text{rad}$ , and the corresponding feedback control voltage variation  $\Delta V$  was  $(0.012 \pm 0.002)$  V, as shown in figure 4. Therefore,  $k_e$  could be obtained as  $(5.6 \pm 1.4) \times 10^{-6}$  N m rad<sup>-1</sup>, which agreed with the theoretical value given by equation (1) and  $k_e / k_f \sim 438$  was deduced.

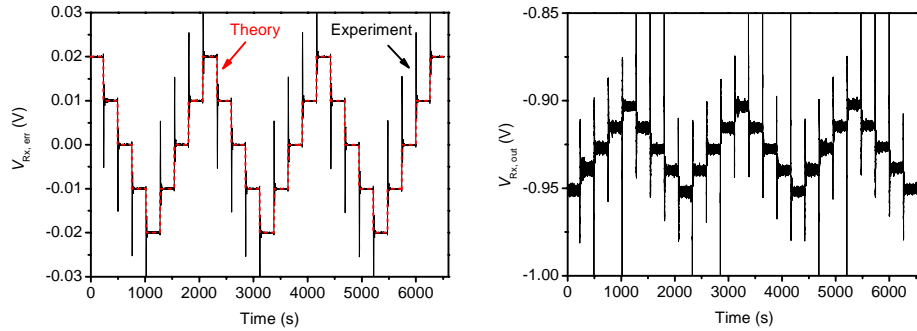


Figure 4 Left: The dash and solid lines respectively represent the expected and experimental error signals. Right: Corresponding control voltage.

### 3.3. Magnetic and thermal disturbance measurement

If assuming the susceptibility  $\chi$  and the residual dipole moment  $\mathbf{M}_r$  are uniform for the whole PM, the torque contributed by the magnetic field of the two coils inside the chamber can be written as

$$\boldsymbol{\tau}_m = \mathbf{M}_r \times \mathbf{B} + \int_V \mathbf{r} \times \nabla [(\mathbf{M}_r/V + \chi\mathbf{B}/2\mu_0) \cdot \mathbf{B}] d\mathbf{v}, \quad (3)$$

where  $\mathbf{B} = \mathbf{B}_1 + \mathbf{B}_2$  is the composite magnetic induction,  $V$  is the volume of the PM, and  $\mathbf{r}$  is the displacement vector of  $d\mathbf{v}$ . Thanks to the symmetrical layout of the two small magnetic coils,  $\mathbf{M}_r$  will contribute null torque to the pendulum when the exciting currents in the two coils are same in amplitude but contrary in direction, which allows independent measuring the influence of  $\chi$ .

When the current directions of the two coils were contrary and synchronously changed between 0 A and 0.6 A (typical gradient of magnetic induction was  $7 \times 10^{-3}$  T m<sup>-1</sup> at the center of the PM), the feedback voltage variation  $\Delta V$  was  $(-1.9 \pm 0.3)$  mV and the corresponding torque was  $1.1 \times 10^{-11}$  N m. Based on the numerical calculation of equation (3) with the parameters of the coils, the susceptibility of the PM was measured about  $(4.2 \pm 0.8) \times 10^{-4}$ . When the currents directions of the two coils were

uniform (typical magnetic induction was  $2 \times 10^{-4}$  T at the center of the PM), the feedback voltage variation  $\Delta V$  was  $(1.1 \pm 0.2)$  mV and the coupling torque was  $-6.4 \times 10^{-12}$  N m. Solving equation (3) combining with the values of  $\chi$  and  $M_{tz}$ , the  $Y$  component of  $M_t$  was obtained as  $M_{ty} = (9.5 \pm 1.8) \times 10^{-8}$  A m<sup>2</sup>.

The pair of heaters near  $T_1, T_3$  and another pair of heaters near  $T_2, T_4$  were alternately heated to periodically produce a significant temperature difference  $T_d = (T_1 - T_2 + T_3 - T_4) / 2$  between the electrodes. The temperature modulation experiment showed that the control voltage variation was less than 0.3 mV when the temperature difference  $T_d$  came to 0.55 °C, it means that the temperature coupling factor of the electrostatic torsion pendulum was below  $3 \times 10^{-12}$  N m K<sup>-1</sup>, which was limited by the sensitivity of the electrostatic-controlled pendulum. The upper-limit temperature coupling factor obtained from the preliminary experiments is about 15 times of those of the radiometer and radiation effects predicted [13, 14], which would be carefully investigated in the further experiments.

### 3.4. Coupling measurement between translation and twist motions

Moving the electrode frame along  $Z$  axis in the range of  $\pm 45$   $\mu\text{m}$  by periodically driving the manipulator, as shown on the left in figure 5, the variation of the feedback voltage  $\Delta V$  reflected the coupling came from the translation was shown in the right picture of figure 5. The result showed that the coupling intensity was various as  $(0.5 \sim 5) \times 10^{-11}$  N m  $\mu\text{m}^{-1}$  at different displacement of the translation. A similar result was obtained by the coupling measurement along  $Y$  axis translation. Near the capacitance equilibrium position, the coupling coefficient was about  $2.5 \times 10^{-11}$  N m  $\mu\text{m}^{-1}$ . Main coupling was estimated from the imbalance of the parasitic capacitances derived from conductive wires, which contributed a nonzero angle  $\Delta\theta$  between the PM and the frame, and then produced a coupling torque as  $k_e \times \Delta\theta$ . The coupling from the presence of the stray DC potentials on the electrodes and the spurious motion of the manipulator stage were investigated in the further experiments.

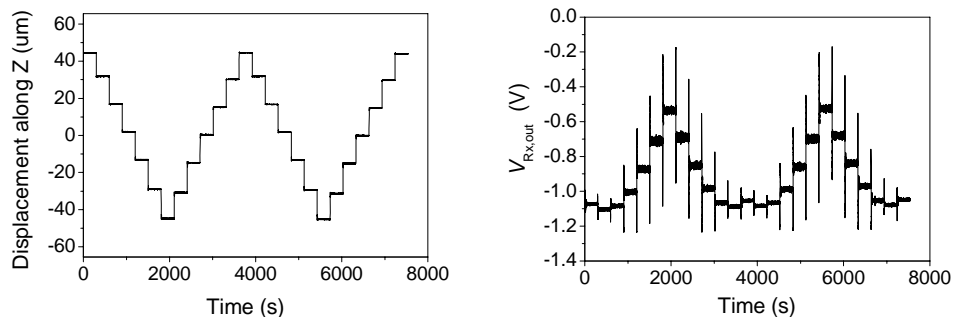


Figure 5 Left: Displacement of the electrode frame along  $Z$  axis. Right: Variation of the control voltage.

### 3.5. Current torque resolution of the controlled pendulum

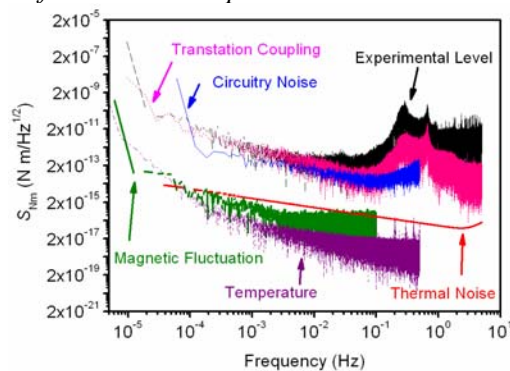


Figure 6 Torque noise of the controlled pendulum.

Feedback voltage as well as the temperature and magnetic field fluctuations of the experimental environment was recorded for a long time. The equivalent torque noise of the controlled pendulum came to  $6 \times 10^{-13} \text{ N m Hz}^{-1/2}$  in the frequency range from 2 mHz to 0.1 Hz, as shown in figure 6, which was mainly limited by the coupling disturbance from the translations seismic noise. The limit due to the capacitance transducer was 3 times lower than the experimental level.

The fluctuations of the temperature and magnetic field of the experimental environment were lower than  $0.03 \text{ }^\circ\text{C} / \text{day}$  and  $5 \text{ } \mu\text{T} / \text{day}$ , respectively. For the ground-based testing of the inertial sensor, the limits of the temperature and magnetic field fluctuations as well as the thermal noise were much lower than the present experimental level.

#### 4. Discussions

If the capacitance gap was extended to 4 mm as LISA Pathfinder, and the DC bias voltage  $V_b$  down to 0.1 V, the parasitic stiffness of the capacitance transducer will sharply decrease by a factor of about  $8 \times 10^4$ , which will significantly suppress the translation-rotation coupling and the back action due to the capacitance transducer. If so, the translation-rotation coupling and the back action torque disturbances would be less than the thermal noise of the pendulum of  $2 \times 10^{-15} \text{ N m Hz}^{-1/2}$  at 1 mHz. For requirement of performance measurement of the PM for LISA, high- $Q$  torsion balances should be developed, for example using fused silica fiber suspension [15].

A torsion balance has been constructed to test the multi-degree-of-freedom control of the PM, and also investigate the cross coupling. In addition, a dual pendulum is being considered to investigate the drag-free control on ground, where one PM should be controlled to track to another PM. It is useful for designing and verifying the drag-free control of LISA and LISA Pathfinder [16].

**Acknowledgments:** This work was supported by the National Natural Science Foundation of China under grants 10675047.

#### References

- [1] Touboul P, Foulon B, Willemenot 1998 *Acta Astronautica* **45** 605
- [2] Mester J, Torii R, Worden P, Lockerbie N, Vitale S and Everitt C W F 2001 *Class. Quantum Grav.* **18** 2475
- [3] Touboul P, Foulon B, Rodrigues M, Marque J P 2004 *Aerosp. Sci. Technol.* **8** 431
- [4] Willemenot W and Touboul P 2000 *Rev. Sci. Instrum.* **7** 302
- [5] Schlamminger S, Choi K Y, Wagner T A, Gundlach J H and Adelberger E G 2008 *Phys. Rev. Lett.* **100** 041101
- [6] Tu L C, Guan S G, Luo J, Shao C G and Liu L X 2007 *Phys. Rev. Lett.* **98** 201101
- [7] Carbone L, Ciani G, Dolesi R, Hueller M, Tombolato D, Vitale S, Veber W J and Cavalleri A 2007 *Phys. Rev. D* **75** 042001
- [8] Hueller M, Cavalleri A, Dolesi R, Vitale S and Weber W J 2002 *Class. Quantum Grav.* **19** 1757
- [9] Carbone L, Cavalleri A, Dolesi R, Hoyle C D, Hueller M, Vitale S and Weber W J 2003 *Phys. Rev. Lett.* **91** 151101
- [10] Carbone L, Cavalleri A, Dolesi R, Hoyle C D, Hueller M, Vitale S and Weber W J 2004 *Class. Quantum Grav.* **21** S611
- [11] Zhou Z B, Gao S W and Luo J 2005 *Class. Quantum Grav.* **22** S537
- [12] Zhou Z B, Qu S B, Tu H B, Bai Y Z, Wu S C, Wan Q Y and Luo J 2008 *Int. J. Mod. Phys. D.* **17** 985
- [13] Hueller M, Armano M, Carbone L, Cavalleri A, Dolesi R, Hoyle C D, Vitale S and Weber W J 2005 *Class. Quantum Grav.* **22** S521
- [14] Pollack S E, Schlamminger S and Gundlach J H 2006 *AIP Conference Proceedings* **873** 158
- [15] Nicolodi D, *An improved torsion pendulum for on-ground verification of the LISA gravitational reference sensor*, poster in 7th LISA conference, 16-20 June, 2008, Barcelona
- [16] Private discussion with Gerhard Heinzel